Bio-Medical Materials and Engineering 26 (2015) S1157–S1168
DOI 10.3233/BME-151412
IOS Press

The detection of long-range correlations of operation force and sEMG with multifractal detrended fluctuation analysis[1]

Fan Li[a], Dongxu Li[b,*], Chunhui Wang[a, e], Shanguang Chen[a], Ming Lv[c] and Miao Wang[d]
[a]*National Laboratory of Human Factors Engineering, China Astronaut Research and Training Center, Beijing, 100094, China*
[b]*School of Aerospace and Materials Engineering, National Defense University, Changsha, 410000, China*
[c]*General Hospital of Armed Police Forces, Beijing, 100039, China*
[d]*Guanghua School of Management, Peking University, Beijing, 100871, China*

Abstract. This paper explores the application of multifractal detrended fluctuation analysis (MF-DFA) on the nonlinear characteristics of correlation between operation force and surface electromyography (sEMG), which is an applied frontier of human neuromuscular system activity. We established cross-correlation functions between the signal of force and four typical sEMG time-frequency domain index sequences (force-sEMG cross-correlation sequences), and dealt with the sequences with MF-DFA. In addition, we demonstrated that the force-sEMG cross-correlation sequences have strong statistical self-similarity and the fractal characteristic of the signal spectrum is similar to 1/f noise or fractional Brownian motion.

Keywords: MF-DFA, operation force signal, sEMG, cross-correlation function

1. Introduction

The correlation between operation force and surface electromyography (force-sEMG) is a substantial problem in physical fatigue mechanism research, rehabilitation training, ergonomics, etc. [1-8]. Compared with other physiological signals measured from the human body, sEMG are relatively weak signals and generated from the activities of the neuromuscular system. They are mainly impacted by physiological and measurement factors. The former group's factors include the level of muscle activity, activity synchronization of motor units, muscle fibers recruitment, and muscle fiber conduction velocity [9, 10].The latter group is affected by factors such as detecting electrode positions, skin temperature, muscle length, and muscle contraction mode [11-13]. sEMG are the result of a number of electrical signals of motor units in time and space in the muscle, and they have been proved by researchers as

[1]Shanguang Chen contributes as equal as the first author and is the co-first author.

[*]Address for correspondence: Dongxu Li, School of Aerospace and Materials Engineering, National Defense University, Changsha, 410000, China. Tel.: 13581717128; Fax: 01066362400; E-mail: 19650769@qq.com.

shown in Figures 1b and 1d that these signals are not in a strictly linear steady-state. However, they illustrate some degree of randomness and instability [4, 5, 14]. Due to the limitations of the power spectrum analysis as shown in Figures 3b and 3c, it is difficult to directly represent quantity for probing the dynamical properties of complex multiple-component physical and physiological systems, thereby making it difficult to understand the underlying mechanisms [15, 16]. Therefore, the use of nonlinear signal analysis methods has become a recent trend in this field. To the best of the authors' knowledge, the experiment results that relate to the regulation of force-sEMG correlations have many different arguments.

In this study, we explore multifractal detrended fluctuation analysis (MF-DFA) to detect long-range correlations of the force-sEMG cross-correlation sequences. MF-DFA is mainly applied for in-depth analysis of small and large fluctuations and/or a broad probability density function. Moreover, it indicates sequence correlation by accelerated power-law attenuation and reveals the dependence of the sequence in time scale patterns [17-21]. The MF-DFA method provides a systematic means to identify and quantify the long-range correlations in data sequences obtained from various settings [22-24]. Nevertheless, such reliable analysis from MF-DFA cannot be achieved by using traditional methods. For example, power-spectrum calculations assume that the sequence is stationary. Once they are applied to unstationary time-series, they will lead to misleading results [4, 5, 14].

One purpose of this study was that, we validated the effectiveness of the MF-DFA method for extracting the scaling properties of fluctuations in force-sEMG cross-correlation sequences. Furthermore, it allowed us to avoid the assumptions of linearity and low-dimensional chaos [22, 23]. Another purpose of this study was to investigate the nonlinear characteristics of force-sEMG cross-correlation sequences, and to discuss the different Hurst index values between force signals and four typical sEMG time-frequency domain index sequences at different experiment yields.

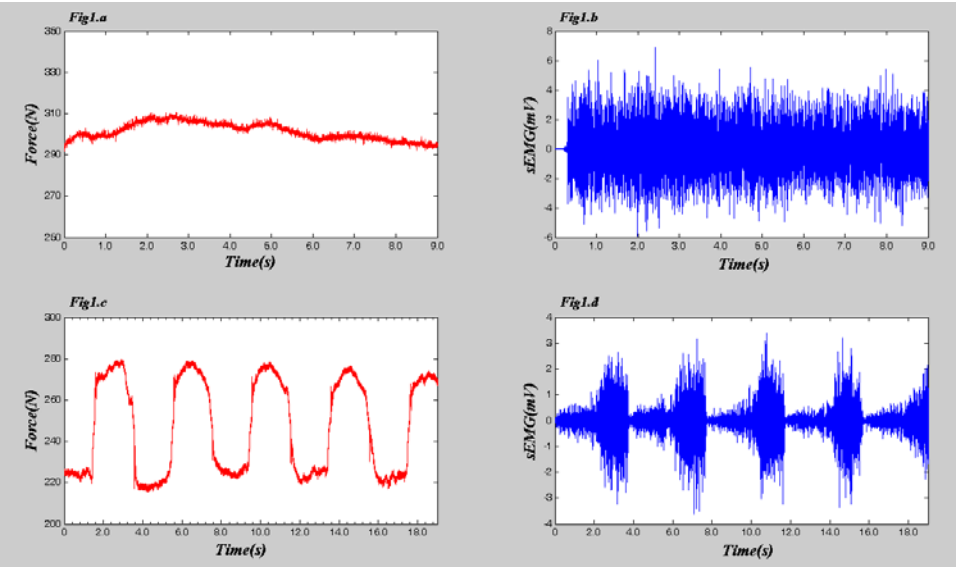

Fig. 1. Consecutive force (red line) and sEMG (blue line) signals are plotted in the columns of volt values versus time. They are recorded from the No. 7subject, who doesisometric exercise (a & b) and isotonic exercise (c & d) at 50% MVC by "BioVision" physiological signal acquisition system (BioVision, Inc.). The sampling frequency is1 KHz.

2. Materials and methods

All human- and animal-related experiment protocols were reviewed and approved by the Institutional Ethical Committee at the National Key Laboratory of Human Factors Engineering.

2.1. Subjects

A total of 21 young male volunteers (age 22.1 ± 2.1 years, height 176.3 ± 2.3cm, weight 68.9 ± 3.4 kg) and 6 middle-aged male volunteers (age 41.3. 8 ± 3.3 years, height 170.3 ± 1.1cm, weight 81.5 ± 1.4 kg) participated in this experiment [25]. They were in good health, and they did not experience muscle fatigue or strenuous exercise in 24 hours before the experiment. They agreed to participate and were familiar with a variety of experimental methods and requirements.

2.2. Experimental method

We carried out the experiment in a double-blind method and studied force-sEMG correlation of upper limb activities in a standard experiment mode. We used step contraction, which is characterized by giving enough time during incremental exercise at different load levels to effectively eliminate fatigue factors. In the experiment, the exercising muscles are retained isometrically and isotonically by constant force, which reflects the basic features of daily exercise. The details are as follows:

(1) The object arm was flexed at an angle of 45°. The angle between the arm and forearm was set to 135° and there was supination of forearm at 30°. The wrist was in neutral position. During the experiment, no support and rotation were given to the arm [26, 27] in Figure 2.

(2) Each volunteer was given four levels of exercise loads, which were 10% maximum volunteer contraction (MVC), 30% MVC, 50% MVC, and 80% MVC. To eliminate the practice effect, subjects performed different load exercises randomly. The exercise was terminated when the subject's Borg fatigue index (BFI) exceeded 6.

(3) Each of these exercises was repeated three times.

Fig. 2. Upper limb location. The arm is flexed at an angle of 45°. The angle between the arm and forearm is set to 135° and there is supination of the forearm at 30°. The wrist is in a neutral position. There is no abduction orrotation in the arm.

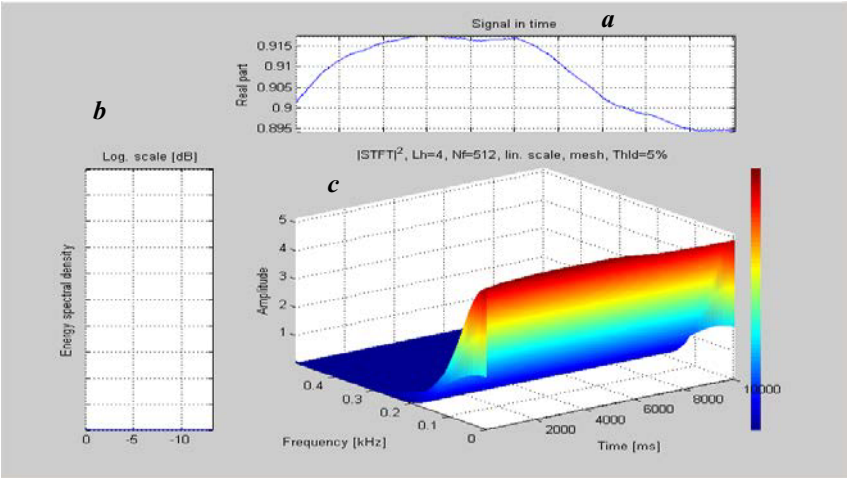

Fig. 3. The cross-correlation sequence, achieved from No. 7 object's 50% MVC isotonic exercise force signal and biceps MPF signal, is analyzed by short time Fourier transform (STFT) with a Hamming window h of 513 points: (a) the signal of cross-correlation in time-domain; (b) energy spectral density of the signal; (c) the signal is visualized a time-frequency representation with pseudo-color plot.

2.3. Data acquisition and processing

2.3.1. The measurement of sEMG

Force signals and sEMGs were recorded by a "Biovision" physiological signal acquisition system (BioVision, Inc.); the sampling frequency was 1 kHz. "3M" surface electrodes were adhered to the surface of each subjects' biceps and triceps parallel with the muscle fibers. The reference electrode was placed on the olecranon bone. Before placing all surface electrodes, the dedicated skin surface was gently smoothed with fine sandpaper and wiped with alcohol cotton balls to clean the remaining keratin and fat. The recorded sEMG signals were filtered by a 20-450 Hz band-pass filter and 50 Hz with its odd harmonics notch filter [28]. Each signal was transformed into two typical sEMG time domain index sequences: Integrated Electromyogram (iEMG) and Root Means Square (RMS), and the frequency domain index sequences: Median Frequency (MP) and Mean Power Frequency (MPF) by Hilbert-Huang Transform (HHT). The four time and frequency indexes reflect the distinctive features of sEMGs from different aspects [9-11]. The correlation between force signal and the four index sequences were studied, which allowed us to distinguish the differences between them.

2.3.2. The establishment of cross-correlation function

The force signal X is determined by $X = \{x(n)\}, n = 0,1,...,N\text{-}1$, and the sEMG index sequence Y is determined by $Y = \{y(n)\},\ n = 0,1,...,N\text{-}1$.

First, the cross-correlation function can be expressed as follow equation:

$$\hat{R}_{XY}(m) = \begin{cases} \sum_{n=0}^{N-|m|+1} x(n)y^*(n+m), & m \geq 0; \\ \hat{R}^*_{YX}(-m), & m < 0; \end{cases} \tag{1}$$

Second, we normalized the above equation by dividing $\sqrt{x^2(n)*y^2(n)}$, which gives:

$$\tilde{R}_{XY}(m) = \hat{R}_{XY}(m) \Big/ \sqrt{x^2(n)*y^2(n)} \quad (2)$$

According to Eqs. (1) and (2), the cross-correlation sequence $\tilde{R}_{XY}(m)$ is a proportional coefficient sequence. The absolute value of $\tilde{R}_{XY}(m)$ indicates that the degree of correlation and the positive or negative value of $\tilde{R}_{XY}(m)$ designates the associated direction.

Third, the value of the maximum correlation and its delay, called the maximum correlation delay (MCD), can be derived by using Eqs. (1) and (2). From the spectrum analysis of the cross-correlation sequence, the range of the maximum delay of in Eq. (1) is reset as twice the MCD of the sequence.

Finally, by utilizing the new MCD value and repeating steps 1 and 2, the new cross-correlation sequence is achieved as shown in Figure 3a. Using the analysis procedures described above, this process allows us to reduce a large number of invalid points of the sequence for the nonlinear analysis in the next step. In addition, since we recorded two types of physiological signals from the time synchronization signal acquisition system, the large time delay was no longer meaningful in force-sEMG correlations.

2.3.3. Nonlinear analysis of cross-correlation sequence

In the previous section, we produced the target force-sEMG cross-correlation sequences. In this part, they are analyzed by the MF-DFA method [22], and we calculate Hurst exponent (H), where H is called the scaling exponent (a self-affinity parameter representing the long-range power-law correlation properties of the sequence). In the case of short-range or even no correlations at all, the detrended walk is similar to a standard random walk (i.e. white noise) and H=0.5. On the other hand, if H<0.5, the correlation in the sequence is not consistent, and an increment is very likely to be followed by a decrement, and vice versa. Moreover, there is more fluctuation of the sequence when H approaches 0. However, when H is any value between 0.5 and 1, the correlation in the sequence is more consistent; an increment is very likely to be followed by another increment, and vice versa. Correspondingly, when it approaches 1, the sequence is even more consistent. Furthermore, if H is equal to1, the sequence is 1/f noise; if H is more than 1.5, the sequence is the typical fractional Brownian motion [22-24].

3. Results

Tables 1 and 2 show the statistical results (mean ± standard deviation) of the Hurst exponent with two types of force-sEMG cross-correlation sequences analyzed by the MF-DFA method [22, 29]. Those results demonstrate that the correlation sequences between the operation force and sEMG have strong statistical self-similarity as shown in Figure 4, and their fractal characteristics of the signal spectrum is similar to 1/f noise or fractional Brownian motion [30]. In summary, they indicate three features of the force-sEMG cross-correlation sequence as follows:

(1) MF-DFA provides a systematic means to identify and quantify the long-range correlations in force-sEMG cross-correlation sequences obtained from various settings. To a determined K-order polynomial (K), the generalized Hurst exponent H (q) is a solodecreasing function that always decreases as q increases. Thus, the force-sEMG cross-correlation sequences have mon-

ofractal fractal characteristics. Monofractal signals are homogeneous and have the ‘‘linearity’’ property [31].

Table 1

Hurst exponent statistics by MF-DFA

ITEM	***FORCE VS iEMG***			
	K=1	***K=2***	***K=3***	***K=4***
q=-7	2.4645±0.2201	2.1690±0.2469	2.1946±0.2485	2.2394±0.2665
q=-6	2.4386±0.2183	2.1506±0.2458	2.1784±0.2476	2.2241±0.2648
q=-5	2.4029±0.2148	2.1282±0.2438	2.1596±0.2460	2.2069±0.2623
q=-4	2.3514±0.2075	2.1014±0.2404	2.1390±0.2435	2.1884±0.2592
q=-3	2.2736±0.1915	2.0711±0.2359	2.1179±0.2402	2.1705±0.2560
q=-2	2.1582±0.1567	2.0401±0.2336	2.0989±0.2372	2.1555±0.2540
q=-1	2.0329±0.1084	2.0150±0.2395	2.0841±0.2367	2.1446±0.2540
q=0	1.9722±0.1097	2.0006±0.2541	2.0746±0.2404	2.1376±0.2562
q=1	1.9440±0.1420	1.9950±0.2715	2.0712±0.2496	2.1341±0.2602
q=2	1.9249±0.1697	1.9912±0.2873	2.0713±0.2617	2.1329±0.2652
q=3	1.9113±0.1869	1.9815±0.2970	2.0701±0.2718	2.1317±0.2700
q=4	1.9009±0.1973	1.9670±0.3010	2.0656±0.2784	2.1290±0.2740
q=5	1.8925±0.2039	1.9517±0.3022	2.0589±0.2824	2.1246±0.2770
q=6	1.8854±0.2086	1.9377±0.3026	2.0512±0.2889	2.1191±0.2839
q=7	1.8793±0.2182	1.9256±0.3025	2.0433±0.2896	2.1132±0.2849
NOTE	The Hurst exponent statistics results (mean±standard deviation) of all experiments’ force-iEMG and force-RMS cross-correlation sequences by MF-DFA are similarly. So there is only listed the force-iEMG cross-correlation sequences statistics.			

Table 2

Hurst exponent statistics by MF-DFA

ITEM	***FORCE VS MPF***			
	K=1	***K=2***	***K=3***	***K=4***
q=-7	2.1032±0.2972	1.7738±0.3877	1.7600±0.3782	1.7601±0.3725
q=-6	2.0845±0.2939	1.7625±0.3867	1.7491±0.3792	1.7493±0.3738
q=-5	2.0612±0.2881	1.7508±0.3850	1.7381±0.3803	1.7385±0.3753
q=-4	2.0316±0.2772	1.7396±0.3824	1.7281±0.3814	1.7289±0.3770
q=-3	1.9943±0.2564	1.7311±0.3788	1.7208±0.3821	1.7218±0.3787
q=-2	1.9502±0.2184	1.7271±0.3744	1.7170±0.3820	1.7181±0.3798
q=-1	1.9198±0.1702	1.7286±0.3696	1.7167±0.3814	1.7172±0.3803
q=0	1.9283±0.1406	1.7362±0.3646	1.7196±0.3800	1.7180±0.3799
q=1	1.9372±0.1379	1.7524±0.3589	1.7258±0.3779	1.7194±0.3785
q=2	1.9357±0.1420	1.7721±0.3540	1.7332±0.3750	1.7203±0.3762
q=3	1.9309±0.1462	1.7857±0.3517	1.7377±0.3717	1.7198±0.3735
q=4	1.9256±0.1499	1.7913±0.3504	1.7383±0.3687	1.7173±0.3707
q=5	1.9203±0.1532	1.7913±0.3493	1.7356±0.3661	1.7130±0.3682
q=6	1.9151±0.1562	1.7880±0.3484	1.7311±0.3638	1.7076±0.3659
q=7	1.9101±0.1587	1.7832±0.3475	1.7255±0.3619	1.7018±0.3641
NOTE	MF-DFA Hurst exponent statistics results of force-MPF and force-MF cross-correlation sequences are similarly. There is only listed the force-MPF cross-correlation sequences statistics.			

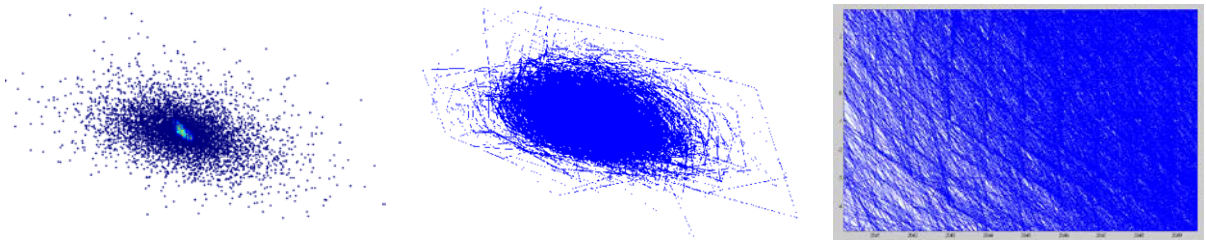

a b c

Fig. 4. Using the reconstruction of phase space to construct the two-dimensional space, we take R_{XY} (m) as abscissa and the derivative of R_{XY} (m) as ordinate for the return map. (a) pseudo-color scatter plot of return map; (b) line plot of; (c) partial enlarged view plot of return map. As can be seen from Figure 4c, R_{XY}(m), the sequence has some the statistical self-similar structures in two-dimensional space trajectory.

Note: In the case that the sequence trajectories tend to one point in reconstructed phase space (the so-called attractor is one point), it indicates that the system is in a steady state; in the case that the trajectories eventually constitute a closed curve (the attractor is a closed curve), it indicates that the system is in a periodic motion; in the case that the trajectories are in a dense, haphazard manner within a limited range, it means that the system is in a random motion; in the case that the distribution of trajectories has some special structure (so-called strange attractor), the system is likely to be in chaos [32].

(2) With showing different average values of MF-DFA Hurst exponents, the nonlinear fluctuation of Type 1 sequences is more obvious than Type 2 sequences by ANOVA at 1% significance level. However, there is no difference in force, and the same type of domain sEMG cross-correlation sequences is observed by utilizing the Scheffe's method for post-hoc procedure analysis. We carried out the normality test, which shows the results are in line with the normal distribution.

(3) When K=4, the range of the Type 1 Hurst exponent is minimizedby comparing it with the results of a different order DFA. It indicates the influence of third-order detrended fluctuation is most significant in Type 1 sequences. In Table 1, it only presents K=1…4, for the higher power order polynomial fitting of DFA; it stops changing with increasing values of K [31, 33]. Similarly, the most dramatic effect in Type 2 sequences is the first-order detrended fluctuations.

4. Discussion

First, the force-sEMG cross-correlation sequences exhibit monofractal behavior (Figure 5). This indicates the presence of nonlinearities and 1/f noise behaviors that are homogeneous and have the same scaling properties in a general level. We believe the cross-correlation sequences are encoded by operation force signals that have more linear properties, and they are characterized by a single singularity exponent h_0 throughout the entirecross-correlation sequence. Therefore, the cross-correlation sequences can also be indexed by a single global exponent—the Hurst exponent $H = h_1$, which suggests that they are stationary from the view point of their local scaling properties [18-21]. However, it is not clear why the value of H ($q<0$) should be bigger than the value of H ($q>0$), whereas H (q) is a monotonically growing function.

Second, the MF-DFA was utilized in this study to accurately quantify long-range power law correlations embedded in non-stationary time series. Even there are segments removed from the series, random spikes or analyzed superposition (e.g., the root mean square) for their correlation are persistent (the scaling exponent $H>0.5$) [32, 35]. With regarding to the fractal characteristic of the signal spec-

trum, it is similar to the 1/f noise or fractional Brownian motion; the cross-correlation sequence $\hat{R}_{XY}(n)$ (to any scale $n>0$) can be approximated by a power-law function, as shown in Eq. (3):

$$\hat{R}_{XY}(n) \propto bn^{\lambda}, n=1,...,N_{\max}, \tag{3}$$

Since the fluctuation function Fq(n) for a power-law trend $\hat{R}_{XY}(n) \propto bn^{\lambda}$ depends on the power λ, we can get:

$$F_q(n) \propto B_q n^{\alpha_\lambda}, \tag{4}$$

Where $\alpha_\lambda = lgF_q(n)$ is calculated from the generalized Hurst exponent H (q) by the MF-DFA method, which is the effective exponent for the power-law trend. According to the reference [29], we know that for any order K of the DFA method, the relation of α_λ and λ can be established by the following expression:

$$\lambda \approx \alpha_\lambda - 1.5 \text{ for } -1.5 \le \lambda \le K - 0.5, \tag{5}$$

By Eq. (10) and the result of H (q), we have:

$$-0.2 < \lambda < 1.3, \tag{6}$$

Eqs. (3) and (6) specify that the fractal spectrum characteristic of the cross-correlation sequence $\hat{R}_{XY}(n)$ is similar to 1/f noise or fractional Brownian motion.

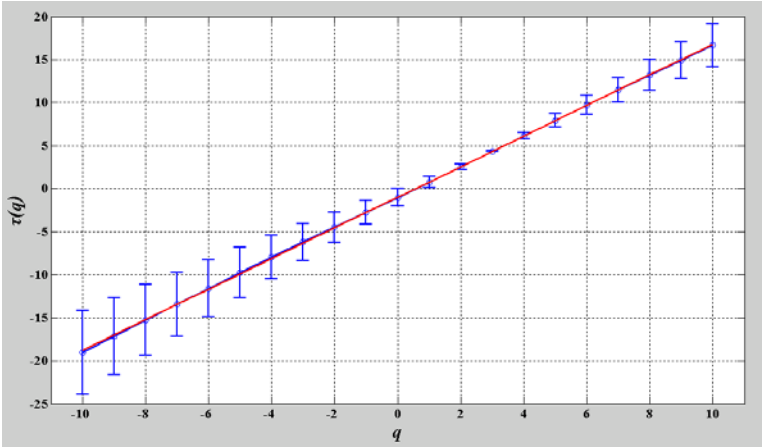

Fig. 5. Multifractal spectrum τ(q) of the Type 1 sequence averaged from 27 subject records. The results show monofractal behavior of the subject force-sEMG cross-correlation sequences. The error bars (vertical blue lines) indicate the standard error of the average τ(q).
Note: Multifractal spectrum τ(q) for individual records. A monofractal signal would correspond to a straight line (red line) for τ (q); for a multifractal signal τ(q) is nonlinear.

Third, well-established linear relationship of *lgFq(n)* (Hurst exponents) and the time scales *lg(n)* can be observed by analyzing log-log plots of *Fq(n)* versus n for each q, and such plots have abrupt change points when *K>1*, as shown in Figure 6. However, the crossover is usually due to a change in the correlation properties of the signal at different time or space scales [36]. This means that as the sequence changes, its fluctuations before and after the time scales corresponded to the abrupt change points. For example, at n=199 and n=466 shown in Figure 6 Hurst exponents exhibit changes in three different phases. For the first phase before n=199, short-term Hurst exponents are bigger than those in the second phase between n=199 and n=466. In the second plateau, the slope of the log-log plot is the smallest among the three phases, which reflects the lack of a power-law scaling behavior for this phase. In the third phase, long-term Hurst exponents return to approximately the same level as in the first stage. This suggests that the behavior of *Fq(n)* is dominated by the segments exhibiting lower positive correlations in the case that their fixed size of the relative fraction in the signal is about 199-466 points. Physically, cross-correlation sequences are intrinsically related to the two-phase muscle movement phenomena. In fact, it is based on sliding filament theory of muscle [37] that the actomyosin movements observed are introduced by resonant dynamics between concentric contraction and eccentric contraction. Consequently, the concentric contraction leads to a significant fluctuation in the first and third phases. Regarding the effects of eccentric contraction, which is in the second plateau, the lack of a power-law scaling behavior is detected as no muscle tension. This demonstrates that extreme changes in the two-phase flow pattern induce the large fluctuations of cross-correlation sequences (low- and high-frequencies).

In addition, Figure 6 shows that the 1st-3rd order fluctuation components in the sequence increase and decrease in the 0.1990s-0.4660s cycle. In this period, the sequence correlation is the smallest. On the other hand, additional evidence can be found in Figures 3b and 3c that it is very consistent to show that spectral principal components of the sequence signal power are concentrated at around 5 Hz. As shown in some studies [16-21], many physical and physiological signals exhibit that the invariant feature is characterized by 1/f scaling and long-range power-law correlations in complex scales. This kind of feature suggests that dynamical processes influenced by input and feedback on multiple time scales could be sufficient to give rise to 1/f scaling and scale invariance [37-40]. Previously, it has been revealed that the signals are monofractal and homogeneous. However, we have demonstrated the sEMG and its correlation series are multifractal signals. Thus, they are nonlinear and inhomogeneous with local properties changing with time. Such signals also can be characterized by different Hurst exponents as q changes. Since the value of the Hurst exponents is over 1, it reflects that they are similar as heartbeat fluctuations that are primarily controlled by the involuntary (autonomic) nervous system [18, 19, 28, 29]. In contrast, the voluntary muscle contraction is an automatic-like process, and voluntary inputs play a major role. The control is based on a multiple-component nonlinear feedback mechanism encompassing coupled neuronal nodes located in the central and peripheral nervous systems, with each system acting in a specific range of time scales [20, 30, 31].The system arises from layers of neural control with multiple component interactions, and exhibits temporal organization over multiple time scales. The muscle fibers' voluntary contraction is similar to interacting input in the force product stochastic model. Through multiple feedback loops, it may be imprinted in their nonlinear and multifractal features.

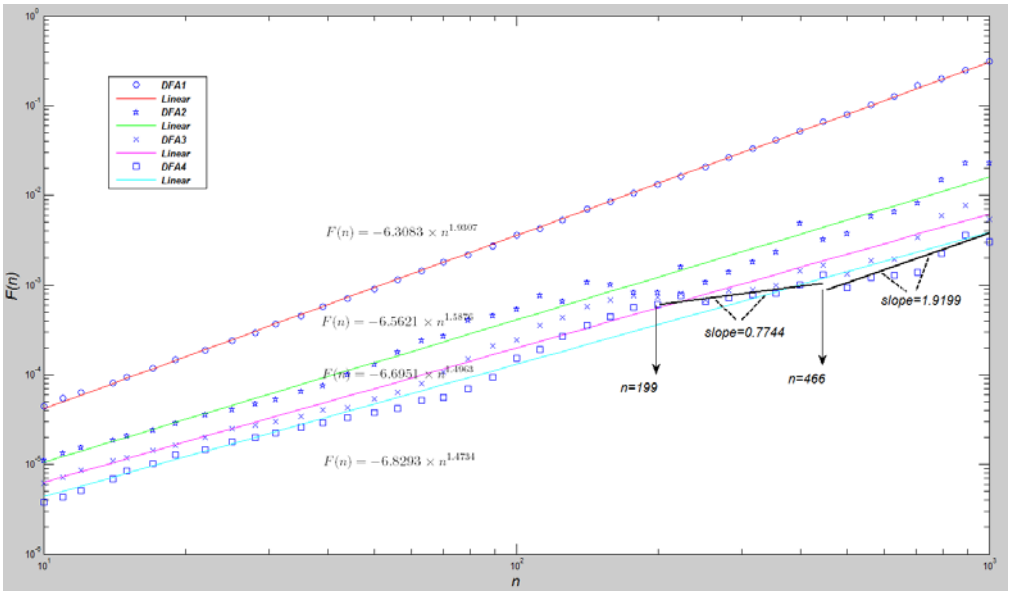

Fig. 6. Double-logarithmic plot of Fq=$2^{(n)}$vs n for the cross-correlation sequence achieved from No. 7 object's 50%MVC isotonic exercise force signal and biceps MPF signal (other consequences have the same characteristics.)
Note: Different order DFA1-4 (for K=1, 2, 3, and 4) differ in their capability to eliminate trends in the series (order K-1 in the original series).

5. Conclusion

In this work, we present that the MF-DFA method can potentially contribute to the investigation of the fluctuation and correlation of complex physiological signals. The transformed sequences can be filtered out to achieve the trend of their own evolution ingredients, and the main fluctuations ingredients is in the rest of the deviation sequences. However, the physiological relevance of the present findings was addressed briefly in this paper due to the scale and limitation of this study, but such work has been planned in a further study in the near future. We will be required to identify whether the precise force-sEMG correlation function expression can be used for force signal measurement, and for the development of new models [2, 3] that could account for the scale-invariant outputs for different types of feedback systems.

Acknowledgments

This work is supported by National Basic Research Program of China (973 Program No. 2011CB711000), the National Natural Science Foundation of China (Grant No. 31400843) and Advanced Space Medico-engineering Research Project of China (No. 2013SY54B0701).

References

[1] J.M. Wakeling, S. Sabrina, M. Lee, et al., A muscle's force depends on the recruitment patterns of its fibers, Annals of Biomedical Engineering **40** (2012), 1708-1720.

[2] C.J. De Luca, A. Adam, et al., Decomposition of surface EMG signals, Journal of Neurophysiology **96** (2006), 1646–1657.
[3] S.H. Nawab, S.S. Chang and C.J. De Luca, High-yield decomposition of surface EMG signals, Clinical Neurophysiology **121** (2010), 1602–1615.
[4] O. Bida, D. Rancourt and E.A. Clancy, Electromyogram (EMG) amplitude estimation and joint torque model performance, IEEE 31th Annual Northeast Bioengineering Conference, Apr. 2005, pp. 229-230.
[5] Lukai Liu, Pu Liu, et al., System identification of non-linear, dynamic EMG-torque relationship about the elbow, IEEE 37th Annual Northeast Bioengineering Conference, Apr. 2011, pp. 1-2.
[6] Wanxiang Yao, R.J. Fuglev and R.M. Enoka, Motor-Unit synchronization increases EMG amplitude and decreases force steadiness of simulated contractions, Journal of Neurophysiology **83** (2000), 441-452.
[7] J.G. Semmler, J.W. Steege, et al., Motor-Unit synchronization is not responsible for larger Motor-Unit forces in old adults, Journal of Neurophysiology **84** (2000), 358-366.
[8] A.M. Taylor, E.A. Christou and R.M. Enoka, Multiple features of Motor-Unit activity influence force fluctuations during isometric contractions, Journal of Neurophysiology **90** (2003), 1350-1361.
[9] G.M. Hagg, Interpretation of EMG spectral alterations and alteration indexes at sustained contraction, European Journal of Applied Physiology **73** (1992), 1211-1217.
[10] Yiwei Liu, M. Kankaapaa, et al., EMG recurrence quantifications in dynamic exercise, Biological Cybernetics **90** (2004), 337-348.
[11] D.M. Pincivero, R.M. Campy, et al., Influence of contraction intensity, muscle, and gender on median frequency of the quadriceps femoris, European Journal of Applied Physiology **90** (2001), 804-810.
[12] S.H. Roy, G. De Luca, et al., Electro-mechanical stability of surface EMG sensors, Medical & Biological Engineering &Computing **45** (2007), 447-457.
[13] A. Rainoldi, G. Melchiorri and I. Caruso, A method for positioning electrodes during surface EMG recordings in lower limb muscles, Journal of Neuroscience Methods **134** (2004), 37-43.
[14] G. Filligoi, F. Felici, et al., Detection of hidden rhythms in surface EMG signals with a nonlinear time-series tool, Medical Engineering & Physics **21** (1999), 439-448.
[15] D. Farina, R. Merletti and R.M. Enoka, The extraction of neural strategies from the surface EMG, European Journal of Applied Physiology **96** (2004), 1486-1495.
[16] A.J. Seely and P.T. Macklem, Complex systems and the technology of variability analysis, Critical Care **8** (2004), 367-384.
[17] E. Bacry, J. Delour and J.F. Muzy, Multifractal random walks, Physical Review E **64** (2001), 6103-6106.
[18] P.Ch. Ivanov, L.A.N. Amaral, A.L. Goldberger, et al., Multifractality in human heartbeat dynamics, Nature **399** (1999), 461-465.
[19] L.A.N. Amaral, P.Ch. Ivanov, N. Aoyagi, et al., Behavioral-independent features of complex heartbeat dynamics, Physical Review E **86** (2001), 6026- 6029.
[20] L. Xu, P.Ch. Ivanov, et al., Quantifying signals with power-law correlations: A comparative study of detrended fluctuation analysis and detrended moving average techniques, Physical Review E **71** (2005), 1101-1115.
[21] P.Ch. Ivanov, J.Q.D.Y. Ma, et al., Levels of complexity in scale-invariant neural signal, Physical Review E **79** (2009), 041920-041931.
[22] J.W. Kantelhardt, S.A. Zschiegner, et al., Multifractal detrended fluctuation analysis of nonstationary time sequences, Physica A **316** (2002), 87-114.
[23] J.W. Kantelhardt, E. Koscielny-Bunde, et al., Detecting long-range correlations with detrended fluctuation analysis, Physica A: Statistical Mechanics and its Applications **295** (2001), 441–454.
[24] D. Vjushin, R.B. Govindan, et al., Scaling analysis of trends using DFA, Physica A: Statistical Mechanics and its Applications **302** (2001), 234-243.
[25] S.M. Kowalski and D.C. Montgomery, Experiments with random factors, in: Design and Analysis of Experiments, 6th ed., John Wiley & Sons, New York, 2009, pp. 93-112.
[26] J.M. Winters and P.E. Crago, in: Biomechanics and Neural Control of Posture and Movement, Springer, New York, 2000.
[27] D. Roman-Liu and T. Tokarski, EMG of arm and forearm muscle activities with regard to handgrip force in relation to upper limb location, Acta of Bioengineering and Biomechanics **4** (2002), 33-48.
[28] Carlo J. De Luca, L. Donald Gilmore, et al., Filtering the surface EMG signal: Movement artifact and baseline noise contamination, Journal of Biomechanics **43** (2010), 1573-1579.
[29] Z. Chen, K. Hu, et al., Effect of nonlinear filters on detrended fluctuation analysis, Physical Review E **71** (2005), 1104-1114.

[30] M. Kobayashi and T. Musha, 1/f fluctuation of heartbeat period, IEEE Transactions on Bio-Medical Engineering **29** (1982), 456-457.
[31] R. Karasik, N. Sapir, et al., Correlation differences in heartbeat fluctuations during rest and exercise, Physical Review E **66** (2002), 2902-2905.
[32] K. Hu, P.Ch. Ivanov, et al., Effect of trends on detrended fluctuation analysis, Physical Review E **64** (2001), 1114-1132.
[33] Q.D.Y. Ma, R.P. Bartsch, et al., Effect of extreme data loss on long-range correlated and anti-correlated signals quantified by detrended fluctuation analysis, Physical Review E **81** (2010), 1101-1117.
[34] Y. Xu, Q.D.Y. Ma, et al., Effects of coarse-graining on the scaling behavior of long-range correlated and anti-correlated signals, Physica A: Statistical Mechanics and its Applications **390** (2011), 4057-4072.
[35] Z. Chen, P. Ch. Ivanov, et al., Effect of nonstationarities on detrended fluctuation analysis, Physical Review E **65** (2002), 1107-1121.
[36] Tingting Gao, Dan Wu, et al., Detrended fluctuation analysis of human EEG during listening to emotional music, Journal of Electronic Science and Technology of China **5** (2007), 272-276.
[37] H.E. Huxley,"The mechanism of muscular contraction," Science,vol. 164, no. 3886, pp. 1356-1366 Jun. 1969.
[38] H.E. Stanley, L.A.N. Amaral, et al., Scale invariance and universality: Organizing principles in complex systems, Physica A: Statistical Mechanics and its Applications **281** (2000), 60-68.
[39] S.B. Lowen, L.S. Liebovitch and J.A. White, Fractal ion-channel behavior generates fractal firing patterns in neuronal models, Physical Review E **59** (1999), 5970-5980.
[40] L.A. Protsmman, H. Meeuwsen, et al., Nonlinear analysis of the scaling properties of human gait: Use of a Hurst exponent as a clinical tool, Psychology of Sport and Exercise **23** (2001), S67-S67.